



Instrument Science Report WFC3 2008-046

WFC3 UVIS Ground P-flats

E. Sabbi, M. Dulude, A.R. Martel, S. Baggett, H. Bushouse
June 12, 2009

ABSTRACT

The Wide Field Camera 3 (WFC3) has two channels, one designed to acquire optical and ultraviolet data (UVIS) and one to operate in the infrared (IR). During WFC3 thermal-vacuum (TV3) testing in 2008, the UVIS20 procedure, “UVIS Flat Fields”, with a total of ~75,000 e- per pixel were acquired in all UVIS filters. These individual flat-fields have been processed into calibration reference flat-fields (P-flats) and installed in the WFC3 pipeline for use with on-orbit data.

Introduction

During spring 2008, WFC3 underwent its third campaign of Thermal Vacuum testing (TV3). Flat fields (UVIS20 procedure) – images taken while the detector is uniformly illuminated – were acquired at the Goddard Space Flight Center as part of the WFC3 calibration plan in all the UVIS imaging filters. The CASTLE Optical Stimulus (OS) system was used to provide flat field illumination of the flight detector UVIS-1'. The IR external flat-field programs in TV3 (IR13S01A and IR13S01B) are discussed separately (Bushouse 2008).

The WFC3/UVIS ground-based reference bias and darks are discussed in Martel et al. (2008a) and Borders (2009), while the python scripts used to generate the entire WFC3/UVIS reference dataset are described in detail in Martel et al. (2008b). In this report we focus on the high-frequency pixel-to-pixel flat-fields (P-flats) and the characteristics of the resulting files. The p-flats have all been delivered to the Calibration Database System (CDBS) and into the archive (MAST).

This ISR is organized as follow: in section 1 we present the data, while section 2 describes how the P-flats were generated. Section 3 discuss how low-frequency flat-fields (L-flats) will further improve the quality of the science data. In section 4 we compare the

Operated by the Association of Universities for Research in Astronomy, Inc., for the National Aeronautics and Space Administration

properties of the P-flats with the requirements listed in the WFC3 Contract End Item (CEI). Conclusions are reported in section 5.

1. Data

During TV3, CASTLE flat-fields were acquired only in the standard configuration of four amplifiers ABCD, gain=1.5 and binning=1x1. Flat-fields with the OS Xenon lamp were taken with the detector at its nominal operating temperature of -82C (IUVDETMP header keyword). A subset of ultraviolet (UV) flat fields has been also acquired at warmer temperature (IUVDETMP=-49C) using the deuterium lamp to achieve higher count rates.

The UVIS channel is equipped with 47 filters and one UV grism. Of the 47 filters, 42 are full-frame filters (18 broad, 8 medium, and 16 narrow-band) while 5 are 'QUAD' filters, where each filter covers 4 different bandpasses, one per quadrant in the field of view.

Similar to ACS, WFC3 has two Main Electronics Boxes (MEB); one has now been chosen as primary for flight (MEB2) while the other is the spare (MEB1). During ground testing, before the flight MEB had been designated, flatfields were acquired using each of the MEBs. To maximize the signal-to-noise in the final P-flats (i.e., at least 75,000 e⁻ total in each filter), all data have been stacked, regardless of MEB used. Comparisons between raw MEB1 and MEB2 flat-fields show that in each quadrant both cold and warm flat-fields differ less than ~0.7%. Ratios of MEB1/MEB2 raw warm and cold flats are shown in Figure 1.

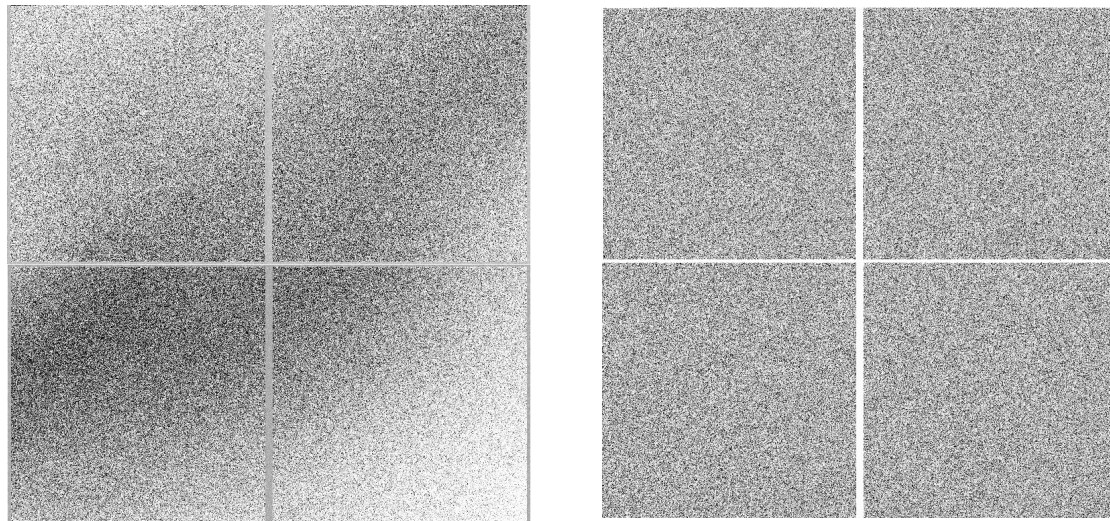


Figure 1: Ratios of MEB1/MEB2 raw flat-fields in the filters F225W (left) and F606W (right) filters. F225W images have been acquired with the detector at -49° C, F606W images at -82° C.

Tables 1 and 2 in Appendix A of this ISR list for each full-frame and quad-filter the raw file name, the temperature, the electronic box, the OS lamp used, and the count rates for all the images used to generate the P-flats.

2. GENERATION OF THE PIXEL-TO-PIXEL FLAT FIELDS

Full-frame filters

For each filter, P-flats were generated with the Python scripts described in Martel et al. (2008b). These scripts process the raw images calling the standard calibration pipeline calwf3¹ (Version 1.3 delivered on March 13th, 2009, also recorded in the reference file header keyword CAL_VER) to calibrate each individual exposure, and then the Pyraf task imcombine is used to stack the exposures for a given filter into a final flat-field.

The calibration switches in the header of the input images determine which calibration steps calwf3 will perform. Similarly the bias and dark reference files used to calibrate the individual flat-field images are selected from the header of the input images. Therefore, before beginning any processing, we updated the header of the raw images with the most-up-to-date reference files and tables.

As a first step, calwf3 initializes the image error (ERR) arrays (extensions 2 and 5) and assigns to each pixel of the raw image an errors (in unit of DN), which depends on bias, gain and readnoise values, listed in the detector calibration parameter table (header keyword CCDTAB, file name *_ccd.fits).

We set the DQICORR=PERFORM in the raw image headers in order to flag known bad pixels and columns into the data quality (DQ, extensions 3 and 6) arrays. At this point calwf3 also looks for saturated pixels in the science (SCI, extensions 1 and 4) arrays. Any pixel value in the SCI arrays that is greater than the SATURATE value listed in the CCDTAB will be flagged in the DQ array. Saturated pixels in the overscan region of the SCI arrays will be also flagged.

CALWF3's next step is to fit the bias level from the CCD overscan regions and subtract it from the image data (BLEVCORR=PERFORM). The boundaries of the overscan regions are taken from the *_osc.fits reference file (header keyword OSCNTAB). Saturated pixels in the overscan regions will be ignored.

Calwf3 subtracts the bias image reference file (header keyword BIASFILE, file name *_bia.fits, see Martel et al. 2008a, header keyword BIASCORR=PERFORM) and then trims the overscan regions from the SCI array.

We set CRCORR to PERFORM to remove cosmic rays (CRs) from the input images. The number of iterations for CR rejection, the sigma levels to use for each iteration, and the spill radius to use during detection are determined by the Cosmic Ray Rejection parameter table (header keyword CRRREJTAB, file name crr.fits). Finally we subtracted the dark image (DARKCORR=PERFORM, DARKFILE=*_drk.fits).

Once all single images from a given filter have been fully processed with calwf3, they were stacked together using the Pyraf task imcombine. The final SCI arrays were normalized to a level of 1.0, with respect to the median value in a 100x100 pixel box of quadrant A (box coordinate x=1032-1133; y=328-429); this region has been chosen because it is relatively free of the “droplet” features (Brown et al. 2008a). In particular, Chip 2 has been divided by the same normalization value as Chip1 to preserve the overall sensitivity difference between the two CCDs. The ERR arrays of the combined images were also normalized to the same scale factor used for the SCI arrays. As done also for

¹ For a detailed description of calwf3 refer to the HST Data Handbook for WFC3 (Kim Quijano et al. 2009)

the dark reference files (Martel et al. 2008b, Borders et al. 2009), and the IR p-flats (Bushouse 2008) the DQ of the flat-field reference files were uniformly set to zero, to avoid the propagation of CR-hit and bad pixels flags into the science data.

The flat-field count rates for both the chips, after they have been normalized, are shown in Figure 2 (broad-band filters) and 3 (intermediate and narrow-band filters). The scale of the y-axis is logarithmic to highlight the number of pixels that are deviating from the mean value. With the exception of the F953N filter, the number of pixels that deviates more than 10% from the mean value is less than 0.7%. In the F593N filter the evident broadening of the mean peak is due to the strong fringing that affects this filter (e.g. Sabbi 2008). With the exception of the warm broad-band flat-fields (Figure 2), in both chip the mean response is 1.0. In the warm broad-band filters, only Chip 1 is peaked at 1.0, while in Chip 2 the peak is at higher values. The difference between the 2 chips is wavelength dependent, and increases toward the UV. This difference is due to the different throughput of the two chips in the UV (Brown 2008b).

All files have been delivered to CDBS and uploaded to the iref directory at STScI. For the most updated list of reference files, consult the web page <http://www.stsci.edu/hst/observatory/cdbs/SIfileInfo/WFC3/reftablequeryindex>.

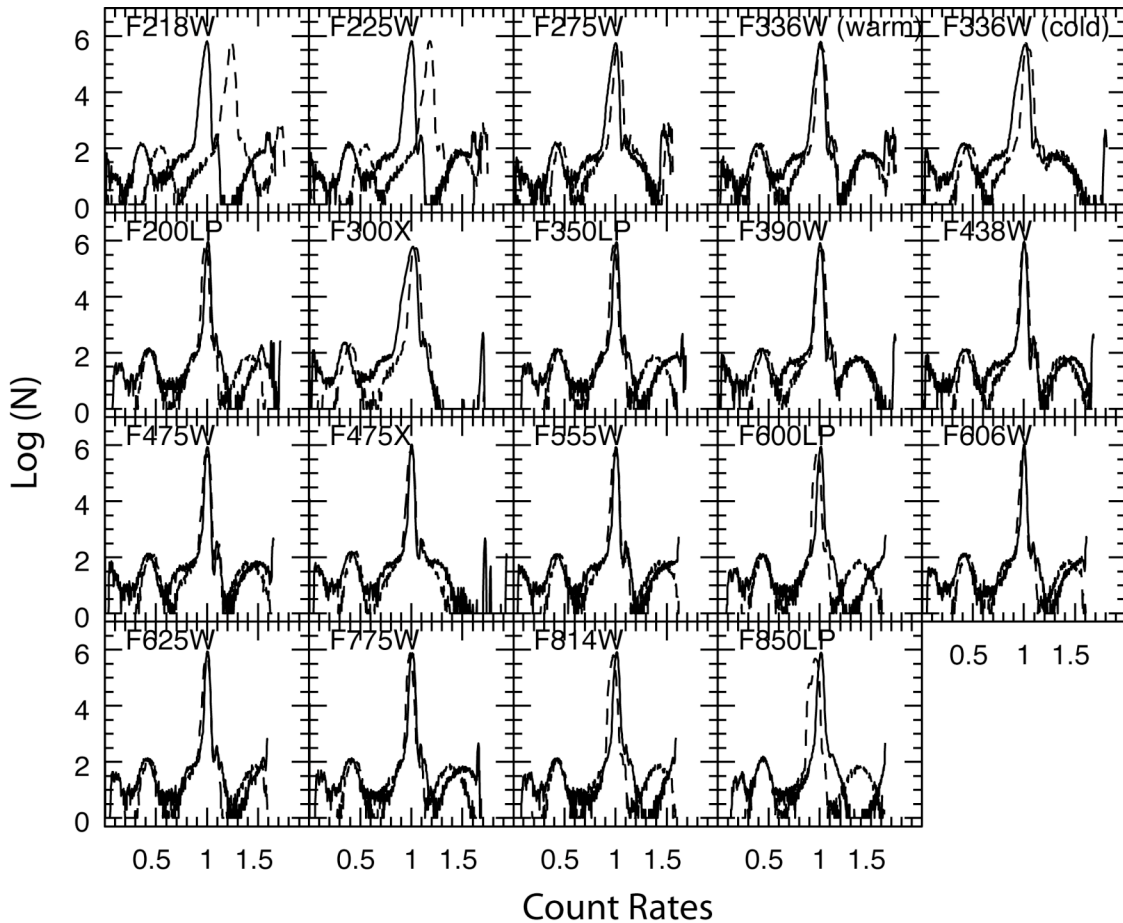


Figure 2: Count rates for Chip1 (continuous line) and Chip2 (dashed line) in broad-band filter P-flats.

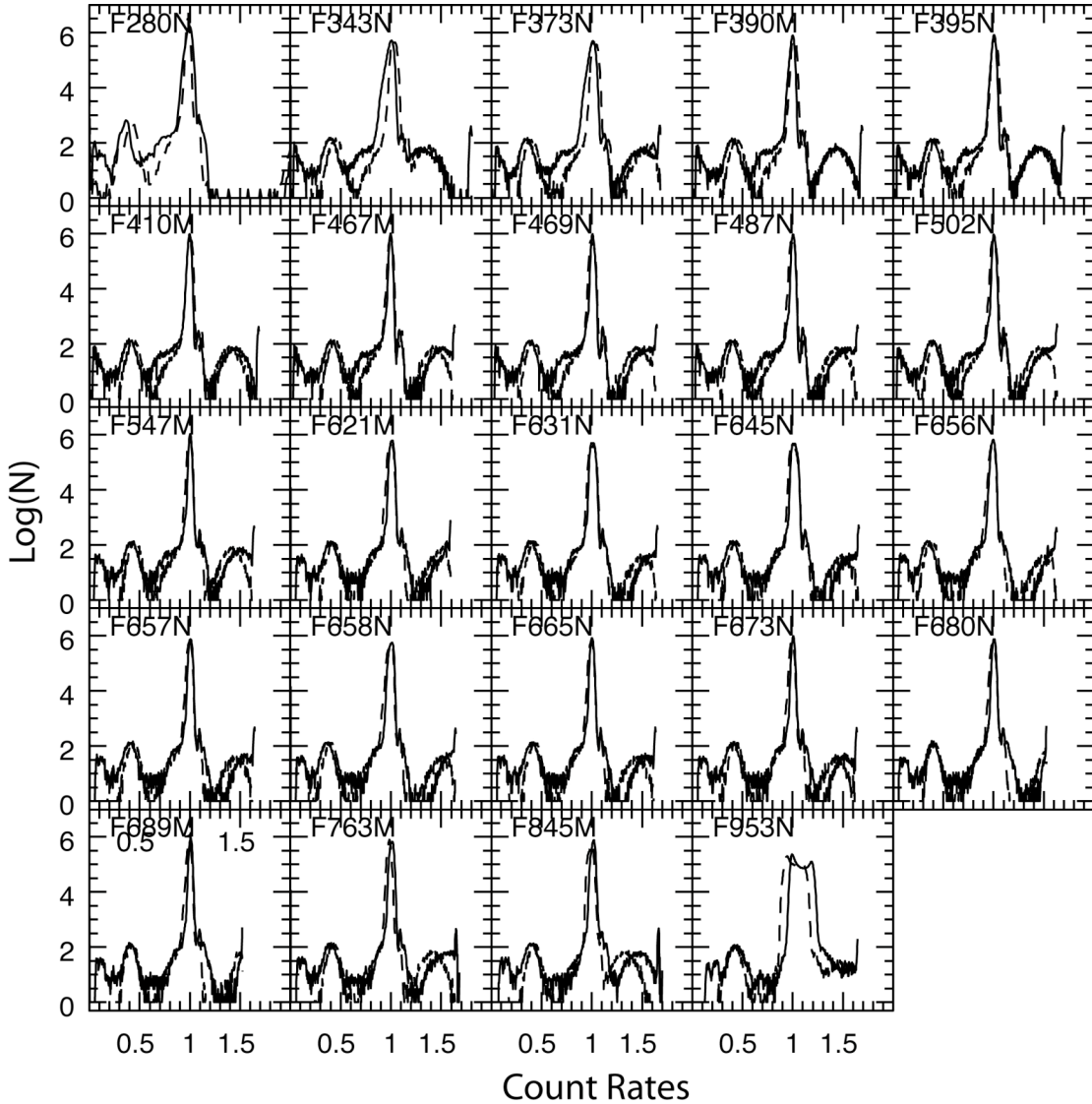


Figure 3: Count rates for Chip1 (continuous line) and Chip2 (dashed line) in intermediate and narrow-band filter P-flats.

Quad filters

As for the full-frame P-flats, quad P-flats were generated using the Python scripts by Martel (2008). For each filter, the individual raw-images were processed with the standard calibration pipeline calwf3, and then stacked together using imcombine.

Because of the different response of the various quadrants of each QUAD filter, each quadrant was normalized to a level of 1.0, with respect to the median value in a 100x100 pixel box of that quadrant (quadrant A x= 456, y= 1585; quadrant B x= 3254, y= 1516; quadrant C x= 1171, y= 974; quadrant D x= 3718, y= 977). These regions were selected to avoid the boundaries between the quadrants and minimize the number of droplet features.

In Quad1 there are three UV filters (FQ232N, FQ243N, and FQ378N) and one optical (FQ437N) bandpass. In order to get enough counts in the UV filters, we acquired

exposures with the deuterium lamp at warm temperature (-49C). In this setup the FQ437N filter is nearly saturated, therefore P-flats for this filter were obtained using the xenon lamp, with the detector at its nominal operating temperature of -82C. As a result, Quad1 is a combination of warm and cold data.

3. L-FLATS.

While the external flat-fields acquired in TV3 contain information about the response of the CCDs and the transmission of the UVIS filters and of the WFC3 optics, they are expected to differ from on-orbit flats because of geometric distortion and the transmission of the HST optics. The differences between the ground and on-orbits flats will be calibrated and removed following the same approach used by the ACS team (Mack et al. 2002, Sirianni et al. 2005): we will observe a moderately dense star fields (in most of the cases ω Centauri) at nine different positions, separated by hundreds of pixels. Fluxes from the same stars will be therefore measured in nine largely separated positions. These data will be fit with a low order polynomial, that will be combined with the ground based flat-fields to remove both the high and the low frequency structures, and to provide a estimate of the chip-to-chip normalization.

Because of variations in the filter transmissions, low-frequency structures will vary as a function of wavelength. During Cycle 17, data will be acquired to directly generate L-flat corrections in several broadband filters. The remaining narrow-, intermediate-, and broad-band low frequency corrections will be obtained through a linear interpolation of the acquired data (see Sabbi et al. 2009 for a description of the observations).

The L-flat will also allow us to improve the quality of the F336W flat-field that is affected by the bowtie, and to correct the effect introduced by the temperature in the warm P-flat.

F336W P-Flat.

Before generating the P-flats, all raw images have been inspected for bowtie anomaly (Baggett et al. 2008), and exposures contaminated by bowties were discarded. The only exception is the filter F336W, where no images without bowtie were found. As a consequence the inverse of this feature will be imprinted on the flat-fielded science data in this filter. This effect will be removed by the low-frequency flat-filed correction (L-flat) that will be determined during SMOV and Cycle 17 by observing 47 Tuc and ω Cen (Sabbi et al. 2009). Because of the bowtie contamination, this filter should not be used to derive L-flat corrections in other filters.

Warm P-flats

As mentioned earlier UV P-flats were generated using data acquired with the detector at a temperature warmer than that used on-orbit. Any differences in the flat-fields due to the temperature differences will be removed by the L-flats, therefore UV ground-based flat-fields will differ from on-orbit flats also because of the different temperature of the detector. These differences will be also removed by the L-flats that will be acquired during Cycle 17.

To quantify the errors introduced by using warm P-flat, we have compared warm P-flats (with good S/N) with cold P-flats (low S/N due to OS limitations). This test indicated that at least half of the displacement between the two peaks in the UV histograms shown in Fig. 1 is due to the different throughput of the two chips in the UV (Brown et al. 2008c), while the remaining half can be attributed to the temperature at which the detector was operated. The warm P-flats will introduce an extra 10% uncertainty in the photometry.

4. CEI VERIFICATION

Ground-based UVIS external flat-fields can be used to verify some of the requirements listed in the CEI.

CCD Detector Uniformity: CEI specification 4.6.11.1 requires that the CCD detector shall be correctable to a uniform gain per pixel to $< 2\%$ at all wavelengths, and $< 1\%$ between 450 and 800 nm. No more than 5% of all pixels shall have response out with $\pm 10\%$ of the mean response.

To verify that the UVIS channel meets this specification we have measured the RMS residuals in single images after new P-flat reference file had been applied, and we found that for all of the UVIS imaging filters, the RMS are $\leq 0.5\%$, and therefore the UVIS channel meets this goal.

Figs. 2 and 3 show that with the exception of the F953N filter, in the full-frame filters no more than 0.7% of all the pixels have response out with $\pm 10\%$ of the mean response, and therefore the UVIS channel meets this goal. The majority of the deviating pixels are in the corners of the images. These features are attributed to the ground system optical stimulus as they are not seen in the internal flat-fields (although the internals do not use all the WFC3 optics). On-orbit data will be used to evaluate the corners.

CCD Detector Low Spatial Frequency Flat-field Structure: CEI specification 4.6.11.2 requires that large scale flat-field uniformities shall not exceed 3% peak to peak including the WFC3 optical system. Existing large-scale uniformities shall be corrected to $< 2\%$. For each filter we have applied the P-flats to one of the raw images. This test showed that all the large-scale structures are correctable to a few tenths of a percent, and therefore the UVIS channel meets this goal.

CCD Detector Non-functional Pixels: CEI specification 4.6.11.3 requires that no more than 1% of the pixels may be non-functional; as shown in Fig.2 and 3, the WFC3 UVIS detectors easily satisfy the expectation.

5. CONCLUSIONS

We have produced a set of full-frame and quad P-flats using ground-based data acquired during TV3. These data will be used to calibration early on-orbit SMOV and Cycle 17 images. On-orbit L-flat data will be used to update the P-flats to fully calibrated science data. An analysis of the ground-based flat-fields shows that the UVIS CCD detectors meet the CEI specifications 4.6.11.1, 2, and 3.

All files have been delivered to CDBS and uploaded to the iref directory at STScI.

Acknowledgments: We thank Jason Kalirai for refereeing this ISR and providing useful suggestions.

References

- Baggett, S., Martel, A.R., Sabi, E., & Deustua, S. 2008, WFC3 ISR 2008-51, “The WFC3/UVIS Bowtie Anomaly”, in preparation
- Borders, T., Baggett, S., Martel, A.R., Bushouse, H. 2009, WFC3 ISR 2009-09, “The WFC3/UVIS Reference Files: 3. Updated Biases and Darks”
- Brown, T., Hartig, G., & Baggett, S. 2008a, WFC3 ISR 2008-09, “WFC3 TV3 Testing: UVIS Window Contamination”
- Brown, T.M. 2008b, WFC3 ISR 2008-48, “WFC3 TV3 Testing: System Throughput on the UVIS Build 1’ Detector”
- Bushouse, H. 2008, WRC3 ISR 2008-28, “WFC3 IR Ground P-Flats”
- Kim Quijano, J., Bushouse, H., & Deustua, S. 2009, “HST Data Handbook for WFC3” Version 1.0 (Baltimore: STScI)
- Martel, A.R., Baggett, S., Bushouse, H., & Sabbi, E. 2008a, WFC3 ISR 2008-42, “The WFC3/UVIS Reference Files: 2. Biases and Darks”
- Martel, A.R., Baggett, S., Bushouse, H. & Sabbi, E. 2008b, WFC3 TIR 2008-01, “The WFC3/UVIS Reference Files: 1. The Script” Available upon request.
- Sabbi, E., et al. 2009, WFC3 ISR 2009-006 “WFC3 Calibration using Galactic Clusters” (in preparation)
- Sabbi E. 2008, WFC3 ISR 2008-12 “UVIS CASTLE Photometric Filter Flat Field Atlas”

APPENDIX A: CHARACTERISTICS OF THE DATA

Table 1: Log of the files used to create the full-frame P-flats. Files marked with an asterisk are affected by the bowtie.

Filter	File	Temperature (C)	Lamp	MEB	Counts (e-)
F200LP	iu200604r_08088133643	-82	Xe	1	39100
	iu200604r_08098190356	-82	Xe	2	41500
	iu200604r_08093223656	-82	Xe	2	42200
F218W	iu201a03r_08055054437*	-49	D2	1	41900
	iu201a03r_08055075437*	-49	D2	1	42200
F225W	iu201a06r_08055060210	-49	D2	1	39900
	iu201a06r_08055081210	-49	D2	1	38800
	iu202106r_08111201444	-49	D2	2	39800
F275W	iu201a02r_08055075437	-49	D2	1	38300
	iu202102r_08111195436	-49	D2	2	38500
F280N	iu201a07r_08055063742	-49	D2	1	19500
	iu201a09r_08055071345	-49	D2	1	19500
	iu201a07r_08055084742	-49	D2	1	19200
	iu201a09r_08055092345	-49	D2	1	19200
F300X	iu200602r_08088133643	-82	Xe	1	19201
	iu200602r_08093223656	-82	Xe	2	24991
	iu200602r_08098190356	-82	Xe	2	24731
F336W	iu200402r_08087212327*	-82	Xe	1	36200
	iu200402r_08092131425*	-82	Xe	2	35700
	iu200402r_08097201126*	-82	Xe	2	34800
	iu202202r_08111141319	-49	D2	2	32900
	iu202202r_08111165419	-49	D2	2	32900
F343N	iu200403r_08087212327	-49	Xe	1	36200

	iu200403r_08097201126	-49	Xe	2	34700
F350LP	iu200606r_08088135611	-82	Xe	1	36600
	iu200606r_08093225649	-82	Xe	2	37900
	iu200606r_08098192349	-82	Xe	2	37300
F373N	iu200405r_08087215226	-82	Xe	1	25635
	iu200405r_08092134324	-82	Xe	2	25330
	iu200405r_08097204025	-82	Xe	2	24689
F390M	iu200409r_08087221016	-82	Xe	1	37800
	iu200409r_08092140114	-82	Xe	2	37400
	iu200409r_08097205815	-82	Xe	2	36500
F390W	iu200407r_08092134324	-82	Xe	2	36500
	iu200407r_08097204025	-82	Xe	2	35700
F395N	iu20040ar_08087222637	-82	Xe	1	24975
	iu20040ar_08092141735	-82	Xe	2	24717
	iu20040ar_08097211436	-82	Xe	2	24115
F410M	iu20040cr_08087222637	-82	Xe	1	37500
	iu20040cr_08087222637	-82	Xe	2	37200
	iu20040cr_08087222637	-82	Xe	2	36300
F438W	iu20040er_08087224144	-82	Xe	1	37500
	iu20040er_08092143242	-82	Xe	2	37200
	iu20040er_08097212943	-82	Xe	2	36500
F467M	iu20040hr_08087225623	-82	Xe	1	38300
	iu20040hr_08092144721	-82	Xe	2	38200
	iu20040hr_08097214422	-82	Xe	2	37400
F469N	iu20040fr_08087225623	-82	Xe	1	38100
	iu20040fr_08092144721	-82	Xe	2	38000
	iu20040fr_08097214422	-82	Xe	2	37200
F475W	iu20040jr_08087231110	-82	Xe	1	38000
	iu20040jr_08092150208	-82	Xe	2	37800
	iu20040jr_08097215907	-82	Xe	2	37100
F475X	iu200607r_08088135611	-82	Xe	1	32300
	iu200607r_08093225649	-82	Xe	2	38000
	iu200607r_08098192349	-82	Xe	2	37200
F487N	iu20040kr_08087232021	-82	Xe	1	38000
	iu20040kr_08092151119	-82	Xe	2	38000
	iu20040kr_08097220818	-82	Xe	2	37100
F502N	iu20040mr_08087233148	-82	Xe	1	38300
	iu20040mr_08092152246	-82	Xe	2	38300
	iu20040mr_08097221945	-82	Xe	2	37300
F547M	iu20040or_08087233148	-82	Xe	1	38100
	iu20040or_08092152246	-82	Xe	2	38100
	iu20040or_08097221945	-82	Xe	2	37300
F555W	iu20040qr_08087234903	-82	Xe	1	41700
	iu20040qr_08092154001	-82	Xe	2	41600
	iu20040qr_08097223700	-82	Xe	2	40900
F600LP	iu200609r_08093231601	-82	Xe	2	37700
	iu200609r_08098194301	-82	Xe	2	37000
F606W	iu20080er_08088062820	-82	Xe	1	38900
	iu208a0dr_08092174744	-82	Xe	2	38900
	iu208a0dr_08098045144	-82	Xe	2	37500
F621M	iu20080hr_08088065959	-82	Xe	1	39500
	iu208a0gr_08092181923	-82	Xe	2	39000
	iu208a0gr_08098052323	-82	Xe	2	38000
F625W	iu20080gr_08088065104	-82	Xe	1	39600
	iu208a0fr_08092181028	-82	Xe	2	39100

	iu208a0fr_08098051428	-82	Xe	2	38100
F631N	iu200802r_08088044930	-82	Xe	1	44100
	iu208a02r_08092162604	-82	Xe	2	37800
	iu208a02r_08098033005	-82	Xe	2	36900
F645N	iu200804r_08088045806	-82	Xe	1	43800
	iu208a04r_08092162604	-82	Xe	2	37500
	iu208a04r_08098033005	-82	Xe	2	36700
F656N	iu200806r_08088053821	-82	Xe	1	44300
	iu208a05r_08092170137	-82	Xe	2	38100
	iu208a05r_08098040537	-82	Xe	2	37300
F657N	iu200808r_08088053821	-82	Xe	1	29523
	iu208a07r_08092170137	-82	Xe	2	25322
	iu208a07r_08098040537	-82	Xe	2	24781
F658N	iu200809r_08088060549	-82	Xe	1	44000
	iu208a08r_08092172552	-82	Xe	2	37500
	iu208a08r_08098042952	-82	Xe	2	36900
F665N	iu20080br_08088060549	-82	Xe	1	44600
	iu208a0ar_08092172552	-82	Xe	2	38100
	iu208a0ar_08098042952	-82	Xe	2	37400
F673N	iu20080dr_08088062820	-82	Xe	1	44600
	iu208a0cr_08092174744	-82	Xe	2	37800
	iu208a0cr_08098045144	-82	Xe	2	37100
F680N	iu20080ir_08088065959	-82	Xe	1	41300
	iu208a0hr_08092181923	-82	Xe	2	40800
	iu208a0hr_08098052323	-82	Xe	2	40100
F689M	iu20080lr_08088072443	-82	Xe	1	41300
	iu208a0kr_08092184414	-82	Xe	2	41000
	iu208a0kr_08098054814	-82	Xe	2	40100
F763N	iu20080mr_08088072443	-82	Xe	1	37200
	iu208a0lr_08092184414	-82	Xe	2	41000
	iu208a0lr_08098054814	-82	Xe	2	37100
F775W	iu20080or_08088074513	-82	Xe	1	37400
	iu208a0nr_08092190447	-82	Xe	2	37800
	iu208a0nr_08098060847	-82	Xe	2	36900
F814W	iu20080pr_08088074513	-82	Xe	1	39200
	iu208a0or_08092190447	-82	Xe	2	39000
	iu208a0or_08098060847	-82	Xe	2	38100
F845M	iu20080rr_08088080332	-82	Xe	1	37200
	iu208a0qr_08092192313	-82	Xe	2	38000
	iu208a0qr_08098062713	-82	Xe	2	37200
F850LP	iu20060ar_08093231601	-82	Xe	2	37500
	iu20060ar_08098194301	-82	Xe	2	36900
F953N	iu208a0rr_08092194752	-82	Xe	2	39500
	iu208a0rr_08098065152	-82	Xe	2	38900

Table 1: Same as Table 1, but for the quad filters

Filter	File	Temperature (C)	Lamp	MEB	Counts (e-)
FQ508N	iu20050cr_08088165348	-82	Xe	1	1222
FQ508N	iu20050er_08088175625	-82	Xe	1	1215
FQ508N	iu20050cr_08095120947	-82	Xe	2	1169
FQ508N	iu20050er_08095131224	-82	Xe	2	1170
FQ674N	iu20050cr_08088165348	-82	Xe	1	4785

FQ674N	iu20050er_08088175625	-82	Xe	1	4785
FQ674N	iu20050cr_08095120947	-82	Xe	2	4777
FQ674N	iu20050er_08095131224	-82	Xe	2	4773
FQ575N	iu20050cr_08088165348	-82	Xe	1	18547
FQ575N	iu20050er_08088175625	-82	Xe	1	18458
FQ575N	iu20050cr_08095120947	-82	Xe	2	17584
FQ575N	iu20050er_08095131224	-82	Xe	2	17608
FQ672N	iu20050cr_08088165348	-82	Xe	1	7167
FQ672N	iu20050er_08088175625	-82	Xe	1	7171
FQ672N	iu20050cr_08095120947	-82	Xe	2	7151
FQ672N	iu20050er_08095131224	-82	Xe	2	7151
FQ437N	iu203A02r_08010043143	-49	D2	2	8162
FQ437N	iu203A04r_08010044344	-49	D2	2	8205
FQ437N	iu203A06r_08010045545	-49	D2	2	8170
FQ437N	iu203A08r_08010050808	-49	D2	2	8220
FQ437N	iu203A02r_08010053943	-49	D2	2	8201
FQ437N	iu203A04r_08010055144	-49	D2	2	8277
FQ437N	iu203A06r_08010060345	-49	D2	2	8142
FQ437N	iu203A08r_08010061609	-49	D2	2	8160
FQ437N	iu203A02r_08010064843	-49	D2	2	8120
FQ437N	iu203A04r_08010070045	-49	D2	2	8174
FQ378N	iu203A02r_08010043143	-49	D2	2	32211
FQ378N	iu203A04r_08010044344	-49	D2	2	32334
FQ378N	iu203A06r_08010045545	-49	D2	2	32175
FQ378N	iu203A08r_08010050808	-49	D2	2	32386
FQ378N	iu203A02r_08010053943	-49	D2	2	32244
FQ378N	iu203A04r_08010055144	-49	D2	2	32533
FQ378N	iu203A06r_08010060345	-49	D2	2	32018
FQ378N	iu203A08r_08010061609	-49	D2	2	32040
FQ378N	iu203A02r_08010064843	-49	D2	2	32003
FQ378N	iu203A04r_08010070045	-49	D2	2	32141
FQ232N	iu203A02r_08010043143	-49	D2	2	2463
FQ232N	iu203A04r_08010044344	-49	D2	2	2442
FQ232N	iu203A06r_08010045545	-49	D2	2	2446
FQ232N	iu203A08r_08010050808	-49	D2	2	2431
FQ232N	iu203A02r_08010053943	-49	D2	2	2426
FQ232N	iu203A04r_08010055144	-49	D2	2	2444
FQ232N	iu203A06r_08010060345	-49	D2	2	2405
FQ232N	iu203A08r_08010061609	-49	D2	2	2406
FQ232N	iu203A02r_08010064843	-49	D2	2	2397
FQ232N	iu203A04r_08010070045	-49	D2	2	2405
FQ243N	iu203A02r_08010043143	-49	D2	2	3520
FQ243N	iu203A04r_08010044344	-49	D2	2	3520
FQ243N	iu203A06r_08010045545	-49	D2	2	3495
FQ243N	iu203A08r_08010050808	-49	D2	2	3507
FQ243N	iu203A02r_08010053943	-49	D2	2	3475
FQ243N	iu203A04r_08010055144	-49	D2	2	3494
FQ243N	iu203A06r_08010060345	-49	D2	2	3439
FQ243N	iu203A08r_08010061609	-49	D2	2	3438
FQ243N	iu203A02r_08010064843	-49	D2	2	3417
FQ243N	iu203A04r_08010070045	-49	D2	2	3425
FQ387N	iu200504r_08088150732	-82	Xe	1	5275
FQ387N	iu200506r_08088152209	-82	Xe	1	5280
FQ387N	iu200508r_08088153646	-82	Xe	1	5284
FQ387N	iu20050Ar_08088155144	-82	Xe	1	5287
FQ387N	iu200504r_08095102332	-82	Xe	2	5016

FQ387N	iu200506r_08095103809	-82	Xe	2	5010
FQ387N	iu200508r_08095105246	-82	Xe	2	5009
FQ387N	iu20050Ar_08095110744	-82	Xe	2	5009
FQ387N	iu200504r_08102033031	-82	Xe	2	4800
FQ387N	iu200506r_08102034508	-82	Xe	2	4795
FQ492N	iu200504r_08088150732	-82	Xe	1	15939
FQ492N	iu200506r_08088152209	-82	Xe	1	15933
FQ492N	iu200508r_08088153646	-82	Xe	1	15933
FQ492N	iu20050Ar_08088155144	-82	Xe	1	15906
FQ492N	iu200504r_08095102332	-82	Xe	2	15978
FQ492N	iu200506r_08095103809	-82	Xe	2	15995
FQ492N	iu200508r_08095105246	-82	Xe	2	16004
FQ492N	iu20050Ar_08095110744	-82	Xe	2	16003
FQ492N	iu200504r_08102033031	-82	Xe	2	15617
FQ492N	iu200506r_08102034508	-82	Xe	2	15626
FQ422M	iu200504r_08088150732	-82	Xe	1	22618
FQ422M	iu200506r_08088152209	-82	Xe	1	22616
FQ422M	iu200508r_08088153646	-82	Xe	1	22623
FQ422M	iu20050Ar_08088155144	-82	Xe	2	22633
FQ422M	iu200504r_08095102332	-82	Xe	2	21961
FQ422M	iu200506r_08095103809	-82	Xe	2	21963
FQ422M	iu200508r_08095105246	-82	Xe	2	21944
FQ422M	iu20050Ar_08095110744	-82	Xe	2	21961
FQ422M	iu200504r_08102033031	-82	Xe	2	20975
FQ422M	iu200506r_08102034508	-82	Xe	2	20953
FQ436N	iu200504r_08088150732	-82	Xe	1	8784
FQ436N	iu200506r_08088152209	-82	Xe	1	8784
FQ436N	iu200508r_08088153646	-82	Xe	1	8788
FQ436N	iu20050Ar_08088155144	-82	Xe	2	8785
FQ436N	iu200504r_08095102332	-82	Xe	2	8563
FQ436N	iu200506r_08095103809	-82	Xe	2	8562
FQ436N	iu200508r_08095105246	-82	Xe	2	8562
FQ436N	iu20050Ar_08095110744	-82	Xe	2	8565
FQ436N	iu200504r_08102033031	-82	Xe	2	8233
FQ436N	iu200506r_08102034508	-82	Xe	2	8222
FQ889N	iu200902r_08088203908	-82	Xe	1	23212
FQ889N	iu200902r_08096032009	-82	Xe	2	22674
FQ937N	iu200902r_08088203908	-82	Xe	1	33764
FQ937N	iu200902r_08096032009	-82	Xe	2	33087
FQ906N	iu200902r_08088203908	-82	Xe	1	26876
FQ906N	iu200902r_08096032009	-82	Xe	2	26258
FQ924N	iu200902r_08088203908	-82	Xe	1	29719
FQ924N	iu200902r_08096032009	-82	Xe	2	29098
FQ619N	iu200905r_08088211423	-82	Xe	1	24993
FQ619N	iu200905r_08096035524	-82	Xe	2	24201
FQ750N	iu200905r_08088211423	-82	Xe	1	22598
FQ750N	iu200905r_08096035524	-82	Xe	2	22006
FQ634N	iu200905r_08088211423	-82	Xe	1	26466
FQ634N	iu200905r_08096035524	-82	Xe	2	25633
FQ727N	iu200905r_08088211423	-82	Xe	1	24201
FQ727N	iu200905r_08096035524	-82	Xe	2	23541